Journal of Hazardous Materials 166 (2009) 998–1005

Contents lists available at ScienceDirect

Journal of Hazardous Materials

journal homepage: www.elsevier.com/locate/jhazmat

Biosorption of lead from aqueous solution by Ficus religiosa leaves: Batch and column study

Suleman Qaiser*, Anwar Rasheed Saleemi, Muhammad Umar

Department of Chemical Engineering, University of Engineering and Technology, Post Code 54890, Lahore, Pakistan

ARTICLE INFO

Article history:
Received 28 July 2008
Received in revised form 1 December 2008
Accepted 1 December 2008
Available online 6 December 2008

Keywords:
Biosorption
Lead
Kinetics
Equilibrium
Thermodynamics

ABSTRACT

The biosorption of lead by Ficus religiosa leaves (FRLs) in powder and immobilized form was investigated. Batch experiments were conducted to determine the biosorption capacity, equilibrium time, optimal pH and temperature. The maximum biosorption capacity of lead was 37.45 mg g^{-1} at optimal pH of 4. The temperature change in the range of 20–40 °C affected the biosorption capacity and the maximum removal was observed at 25 °C. The thermodynamics parameters were determined from experimental data. The Langmuir and Freundlich models were used to explain the equilibrium data. The Langmuir model showed better fit of data with correlation coefficient of 0.97. The kinetics of biosorption followed pseudo second order model. For continuous biosorption experiments, FRLs biomass was immobilized in polysulfone matrix. Breakthrough curves were analyzed at different flow rates, pH and bed depth. Bed depth service time (BDST) and the Thomas models were used to describe the experimental data. A solution of 0.05 M HNO_3 did well to elute lead from biomass. The release of Ca, Mg and Na ions during lead biosorption revealed that ion exchange was the major removal mechanism.

1. Introduction

The contamination of wastewater by toxic metal ions is a worldwide environmental problem. The tremendous increase in the use of heavy metals over the past few decades has inevitably increased the metallic contents in the aquatic environment. Heavy metal ions are of great concern, due to their mobility in natural water ecosystems and due to their toxicity [1]. These metal contaminants are introduced into surface waters through various industrial operations. The pollutants of concern include lead, chromium, zinc, and copper.

Lead is among the most toxic heavy metal ions, affecting the environment [2]. Lead pipes used as drains from the baths, are still in service. Main sources of lead are the manufacture of storage batteries, pigments, leaded glass, mining, metal electroplating, painting, coating, smelting, petrochemical, plumbing fuels, photographic materials, matches and explosives [3,4]. Apart from this lead is also used in insecticides, plastic water pipes, food, beverages, ointments and medicinal concoctions for flavoring and sweetening. These industries discharge lead into the environment without adequate treatment. Untreated effluents from these industries have an adverse impact on the environment and aquatic life [4]. The current Environmental Protection Agency (EPA) standard for lead in wastewater and drinking water is 0.5 and 0.05 mg l^{-1}, respectively [5].

Lead is a toxic metal that is harmful if inhaled or swallowed. Lead can threaten human life due to its toxicity, accumulation in food chains and persistence in nature. Lead has both acute and chronic effects in humans. It may cause anemia, headache, chills, diarrhea and reduction in hemoglobin formation. Lead poisoning causes severe damage to kidneys, nervous system, reproductive system, liver and brain [2,5].

The conventional methods for treatment of lead in wastewater include: precipitation, adsorption with activated carbon, ion exchange, membrane processes, oxidation and reduction [6,7]. These methods are expensive and often involve the use of chemicals and generate large amounts of sludge.

Biosorption is a process that utilizes low cost biosorbents to sequester toxic heavy metals [8]. The advantages of biosorption over the conventional methods are low operating cost, selectivity for specific metal, short operational time and no chemical sludge [9].

Removing metals from wastewater required the use of efficient biosorbent materials. Many agricultural-based waste materials have been employed for the treatment of lead wastes which include: coconut husk and shell [10,11], sea weeds [12,13], sago waste [14], hazelnut shell [15,16], peanut hull [17], tree fern [18], black gram husk [19], maize leaf [20], maize, sun flower waste [21], Oryza sativa L. husk [22], coffee beans [23], Ficus religiosa leaves (FRLs) [24], wheat bran [25], almond shell [16], tea waste [26], etc.

* Corresponding author. Tel.: +92 42 6634068; fax: +92 42 6822566.
E-mail address: engrsqaiser@yahoo.com (S. Qaiser).

0304-3894/$ – see front matter © 2008 Elsevier B.V. All rights reserved.
doi:10.1016/j.jhazmat.2008.12.003

In present research FRLs in free and immobilized forms were utilized for treatment of lead wastes. Effect of temperature, pH and initial metal concentration were investigated. Various thermodynamics parameters, such as ΔH, ΔG and ΔS were evaluated from biosorption data. Column breakthrough data was analyzed using the BDST and the Thomas models.

2. Materials and methods

2.1. Chemicals

Chemicals used were of analytical reagent grade. Polysulfone (Cat No. 18244-3) and n,n-dimethyl-formamide (DMF) were obtained from Aldrich chemicals. Stock lead solution of 1000 mg l^{-1} concentration was prepared by dissolving 1.6 g of lead nitrate (Merck Germany) in 1 l of distilled water. The stock solution was diluted to obtain solutions of various known concentrations of lead. For pH adjustment, 0.1 M nitric acid and 0.1 M ammonia solutions were used.

2.2. Preparation of biosorbent

FRLs were collected locally, from University of Engineering and Technology Lahore, Pakistan. These leaves were washed, repeatedly with tap water to remove dust and soluble impurities and were allowed to dry at room temperature in shadow. The dried leaves were converted into fine powder by grinding in a mechanical grinder. The powder was sieved and the size fraction 60–80 μm was used in the experiments. This powder was soaked in 0.1 M HNO_3 for 24 h (50 g FRLs powder was soaked per litre). The biosorbent was filtered and washed with distilled water to remove acid contents. The washing was continued till the pH of the filtrate was close to 7. It was first dried at room temperature and then in an oven at 105 °C to completely remove moisture. Finally, it was stored in air tight glass bottles to protect it from humidity. Similar treatment of FRLs was performed with 0.1 M $CaCl_2$ solution.

The objective of acid pretreatment is to remove the surface impurities and to expose the binding sites of biosorbent. This pretreatment removed already bound metals from the biosorbent and thus increased its removal capacity. The pretreatment with $CaCl_2$ is performed to prepare the biomass in Ca-form just like an ion exchange resin.

2.3. Immobilization of FRLs

The immobilization of FRLs was performed according to the method of Trujillo et al. [27], but with certain modifications. In an Erlenmeyer flask, 12 g of FRLs biomass was blended into a solution containing 10 g of polysulphone per 100 ml of DMF. The flask was immediately sealed to avoid volatilization of DMF. The mixture was shaken for 24 h on a rotary shaker at 180 rpm to dissolve polysulphone completely in DMF and to form uniform and consistent slurry. The slurry was passed through a syringe into distilled water bath at 6–10 °C. Spherical beads were formed when the atomized slurry contacted with water because of the phase inversion of polysulphone. The biomass was immobilized within the solidified polysulphone matrix. The DMF completely dissolved in water and gradually diffused out which led to the formation of a favorable porous structure for the beads. These beads were cured in distilled water bath, using a stirrer at 120 rpm for 18 h to completely diffuse out DMF. After curing, beads were air-dried for 3 days at room temperature (22–24 °C) and later in an oven at 80 °C, for 6–8 h to completely remove moisture. These beads were screened to obtain a size fraction in the range of 2–3 mm.

2.4. Characterization of biosorbent

Fourier transform infrared (FTIR) spectroscopy was used to identify the functional groups present in the biomass. The biomass samples were examined, using JASCO FTIR spectrometer, within range of 400–4000 cm^{-1}. All analysis were performed using, KBr as back ground material. In order to form pellets, 0.0035 g of FRLs biomass was mixed with 0.3 g KBr and pressed at 6–8 bar. The surface structure and particle size distribution of biosorbent was examined using Hitachi Scanning Electron Microscope (SEM). The samples were covered with a thin layer of gold and an electron acceleration voltage of 20 kV was applied. The surface area, pore volume and pore size measurements of powdered and immobilized biomass were carried out using, Quantachrome NOVA 2200C USA, surface area and pore size analyzer. The gas mixture of 22.9 mol% nitrogen and 77.1 mol% helium was used for this purpose. Multipoint BET and Langmuir surface area was determined. The elemental analysis of the biosorbent was performed using, Costech Instrument 4010, Thermo Jarrel Ash (IRIS, USA) inductively couple plasma atomic emission spectrometer (ICP-AES) and Shimazdu atomic absorption spectrometer.

2.5. Batch biosorption experiments

Batch biosorption experiments were performed by shaking, 0.5 g FRLs biomass with 100 ml lead solution of 100 mg l^{-1} concentration. The shaker was equipped with thermostatically controlled heating water bath, to keep the temperature of the contents to desired levels. After completion of each batch, the solution was filtered, using vacuum filter assembly. The filtrate was analyzed using Shimazdu 6800 atomic absorption spectrophotometer. The amount of lead biosorbed was evaluated by material balance and metal uptake q_t, was calculated [24].

2.6. Fixed bed column experiments

Continuous flow biosorption experiments were conducted in Perspex column of 5.0 cm inside diameter. At the top of the column, an adjustable plunger was attached with a 0.5 mm Perspex sieve. At the bottom of the column, a 0.5 mm Perspex sieve was fixed. The column was packed with 118 g of immobilized FRLs biomass to yield a bed height of 50 cm and a bed density of 120.2 g l^{-1}. Lead solution of 100 mg l^{-1} was pumped to the top of the column, at flow rates of 5–20 ml min^{-1}, using a peristaltic pump. Samples were collected, from the exit of the column at regular time intervals and analyzed for residual lead concentrations. The pH and temperature of the influent and the effluent solutions were measured using Hanna pH meter. Operation of the column was stopped when the effluent lead concentration exceeded a value of 95 mg l^{-1} or higher. The column was then washed with distilled water for several runs. The loaded biomass was regenerated using 0.05 M HNO_3 at flow rate of 10 ml min^{-1}. After elution, distilled water was passed through column to wash the bed until the pH of the wash effluent stabilized near 7.0.

3. Results and discussion

3.1. Characterization of the biosorbent

The FTIR spectra of Ca-treated and lead loaded FRLs is shown in Fig. 1. The FTIR spectra of Ca-treated FRLs, showed the presence of many functional groups, indicating the complex nature of FRLs biomass. A broad band at 3450 cm^{-1} indicates the presence of —OH and —NH groups. The absorbance at 2860 and 2920 cm^{-1} are due to aliphatic stretching. The peak at1656 cm^{-1} is the indication of C=N bending, which further confirms the presence of amino groups.

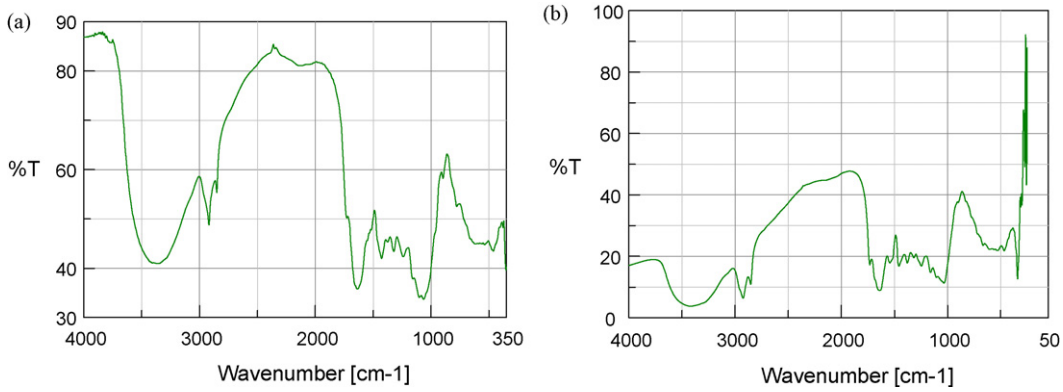

Fig. 1. FTIR spectra of (a) calcium treated FRLs and (b) lead loaded FRLs.

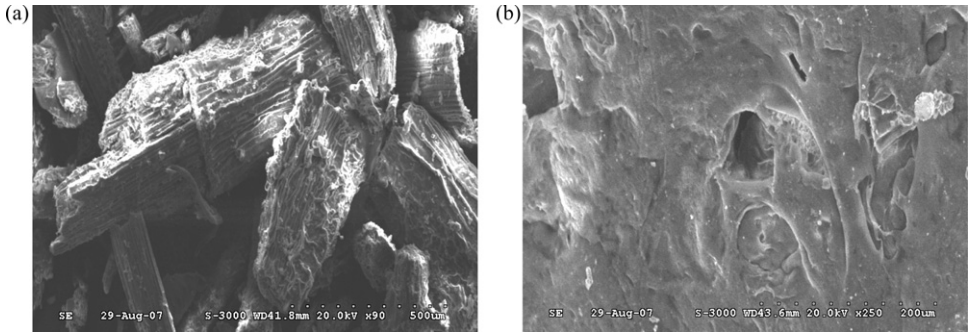

Fig. 2. SEM micrograph of (a) FRLs and (b) immobilized FRLs.

The peak at 1636 cm^{-1} represent C=O. The presence of —OH and C=O, also confirms the presence of carboxylic groups. The peaks appearing in the region 1350 cm^{-1} and 1020 cm^{-1} represents N—H bending and C—OH stretching vibrations, respectively. Absorbance at 1060 cm^{-1} is due to C=O bending. Peak at 1105 cm^{-1} showed the presence of C=S. The FTIR spectra of lead loaded biomass showed increase in the absorption of peaks. The broadness of —OH and C=O peaks indicate the involvement of these groups in the biosorption.

The SEM micrographs of free and immobilized FRLs are shown in Fig. 2. The micrograph in Fig. 2a represents an un-even surface and porous structure of FRLs biomass. The micrograph in Fig. 2b, showed the presence of pores in the immobilized FRLs biomass. The surface area of the biomass further confirmed its porous nature. The surface area and elemental analysis of biosorbent are presented in Table 1.

3.2. Batch biosorption experiments

3.2.1. Determination of equilibrium time

As shown in Fig. 3, the biosorption process took place in two stages. The first rapid stage in which, 60–70% biosorption was achieved in 15 min and a slower second stage, with equilibrium attained in 1 h. The first stage was due to, the initial accumulation of metal at the surface, as large surface area of biosorbent was available. With the gradual occupation of surface binding sites, the biosorption process was slowed down. The second slower stage was due to the penetration of metal molecules to the inner active sites of the biosorbent. This is in accordance with the observations of other similar studies [20,28]. A decrease in pH was observed at the end of the experiments, which may be attributed to the release of H^+ ions, as result of ion exchange between Pb^{2+} and proton. Release of Ca^{2+}, Mg^{2+} and Na^+ was also observed, which further confirmed the exchange of Pb^{2+} ions with light metals present in the biosorbent.

Table 1
Elemental analysis and surface area characterization of biosorbent.

Elemental analysis of FRLs							
Element	C	H	N	S	O		
%Age	48.4	7.3	1.1	0.12	38.4		
Element	Al	Ca	Cr	Fe	Mg	Na	K
%Age	0.22	0.82	0.002	0.032	0.024	0.19	0.12

Surface area and pore size analysis				
	BET surface area ($m^2\ g^{-1}$)	Langmuir surface area ($m^2\ g^{-1}$)	Pore volume ($cm^3\ g^{-1}$)	Pore dia. (Å)
FRLs	6.14	37.76	0.06	123.74
Immob. FRLs	2.98	14.79	0.07	120.50

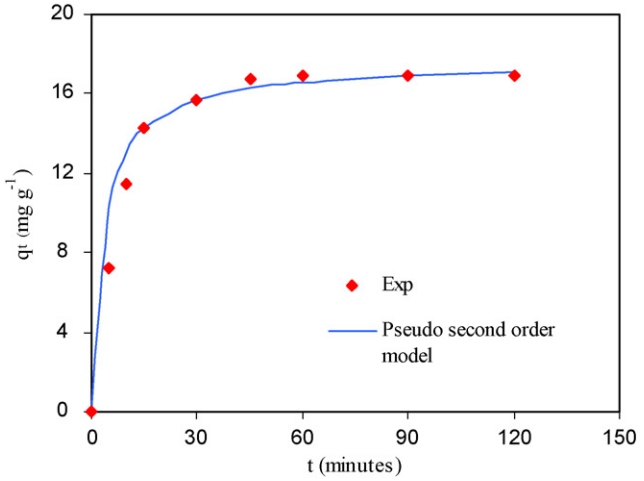

Fig. 3. Kinetics of lead biosorption. Initial conc. = 100 mg l^{-1}, 0.5 g in 100 ml, 26 °C, 200 rpm, pH 5.3.

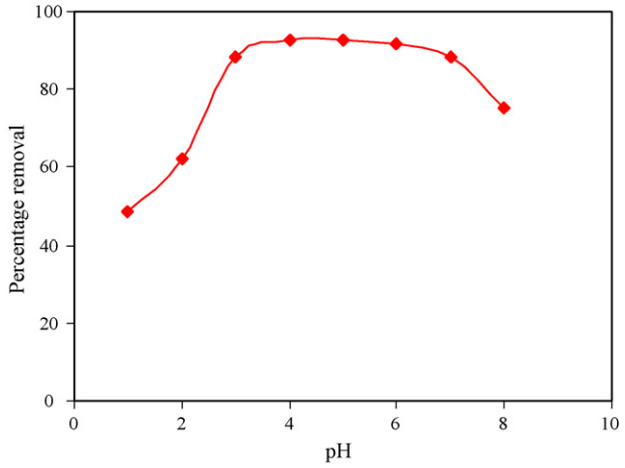

Fig. 4. Effect of pH on lead biosorption. Initial conc. = 100 mg l^{-1}, 0.5 g in 100 ml, 25.4 °C, 200 rpm, 1 h.

3.2.2. Effect of pH

Solution pH plays a vital role in heavy metal biosorption. The speciation of metal in solution is pH dependent and at the same time, the state of chemically active sites is changed by the variation in solution pH. In order to determine the optimal value, pH of solution was varied from 1 ± 0.1 to 8 ± 0.1. As depicted in Fig. 4, the maximum biosorption of lead occurred in the pH range of 3–7. The FTIR results indicated the presence of hydroxyl, carboxylic, carbonyl groups in the FRLs biomass. These groups were protonated at pH values lower than 3.0, and thereby restrict the approach of lead cations to the surface of biosorbent. In the pH range of 3–7 these were negatively charged and facilitate the binding of lead cations. The increase in removal capacity at higher pH may also be attributed to the reduction of H^+ ions which compete with Pb^{2+} ions at lower pH. The speciation of lead is pH dependent. At pH of 2–5 lead always exclusively exists as Pb^{2+}, above pH of 6, it is hydrolyzed to $PbOH^+$ and $Pb(OH)_2$. The predominant sorbing forms of lead are Pb^{2+} and $PbOH^+$ which occurred in the pH range of 4–7. This was the reason for higher removal of lead in the pH range of 4–7. At pH higher than 7, precipitation of lead occurred and removal due to biosorption was reduced.

3.2.3. Biosorption equilibrium

Biosorption equilibrium is established when the concentration of sorbate in bulk solution is in dynamic balance with that on the liquid–sorbent interface. Biosorption isotherms are the equilibrium relationships between the concentrations of biosorbed metal and metal in solution at a given temperature [29].

In the present research, the Langmuir and Freundlich models were utilized to describe the equilibrium data. The Langmuir model is based on the hypothesis that uptake occurs on a homogenous surface by monolayer sorption without interaction between adsorbed molecules, and is expressed as

$$q_e = \frac{q_{max} b C_e}{1 + b C_e} \quad (1)$$

Eq. (1) can be written in linear form as

$$\frac{C_e}{q_e} = \frac{C_e}{q_{max}} + \frac{1}{q_{max} b} \quad (2)$$

where q_{max} represents the maximum biosorption capacity and b is a constant related to affinity and energy of binding sites.

The Freundlich model proposes a monolayer sorption with a heterogeneous energetic distribution of active sites and with interaction between adsorbed molecules. It is expressed mathematically as

$$q_e = K_F (C_e)^{1/n} \quad (3)$$

Linear form of Eq. (3) is

$$\ln q_e = \frac{1}{n} \ln C_e + \ln K_F \quad (4)$$

where K_F and n are the Freundlich coefficients. K_F provides an indication of the adsorption capacity and n is related to the intensity of adsorption.

Initial concentration of lead was varied, from 10 to 1000 mg l^{-1} and quantity of biosorbent was kept constant at 0.5 g. Equilibrium concentration, C_e and equilibrium capacity, q_e were determined in each case. In order to apply the Langmuir model, C_e was plotted against C_e/q_e and straight line was fitted by regression. The correlation coefficient of 0.97 indicated the applicability of the Langmuir model. The values of q_{max} and b were determined from the slope and intercept of the plot. In order to see the applicability of the Freundlich model $\ln C_e$ was plotted against $\ln q_e$. The correlation coefficient of 0.67 was indication of the fact that sorption did not follow the Freundlich model. The Freundlich model constants were determined from the slope and intercept of plot. The values of the Langmuir and Freundlich models constants are listed in Table 2.

The applicability of the Langmuir model to the experimental data indicate that biosorption of lead(II) on FRLs occurred in a monolayer. Fig. 5 shows the comparison of the Langmuir and Freundlich models with the experimental data.

Table 2
Langmuir, Freundlich, pseudo second order, thermodynamics, Thomas and BDST models parameters.

The Langmuir model parameters		
q_{max} (mg g^{-1})	b (l mg^{-1})	R^2
37.45	0.022	0.97

The Freundlich model parameters		
n	K_F	R^2
2.8	3.8	0.67

The pseudo second order model parameters				
T (°C)	K_d (l g^{-1})	K (g mg^{-1} min^{-1})	q_e (mg g^{-1})	R^2
20	3.36	0.012	19.76	0.99
30	1.05	0.016	17.36	0.99
40	0.15	0.025	9.09	0.99
50	0.092	0.019	6.72	0.99

The thermodynamics parameters				
T (°C)	ΔH (kJ mol^{-1})	ΔS (kJ mol^{-1} k^{-1})	ΔG (kJ mol^{-1})	R^2
20	−105.9	−0.35	−2.95	0.96
30			−0.12	
40			4.94	

The Thomas model parameters			
Flow rate (ml min^{-1})	q_o (mg g^{-1})	k_{th} (l mg^{-1} h^{-1})	R^2
5	16.42	0.00085	0.94
10	15.56	0.0016	0.95
20	13.43	0.0037	0.99

The BDST model parameters		
N_o (mg l^{-1})	k_a (l mg^{-1} h^{-1})	R^2
1756	0.0026	0.98

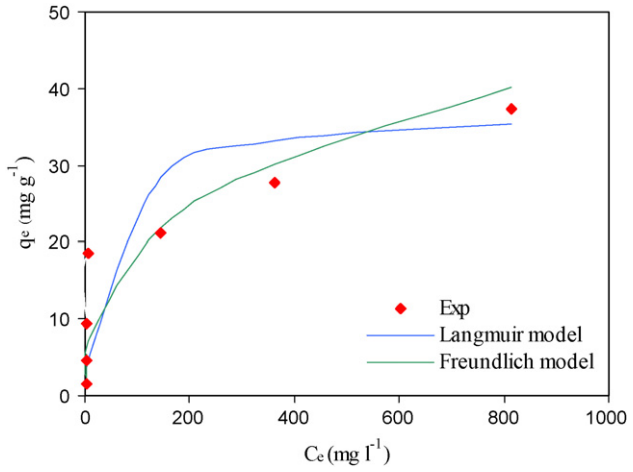

Fig. 5. Langmuir and Freundlich isotherms plot for lead biosorption. Initial conc. = 10–1000 mg l^{-1}, 0.5 g in 100 ml, 25 °C, 200 rpm, 1 h.

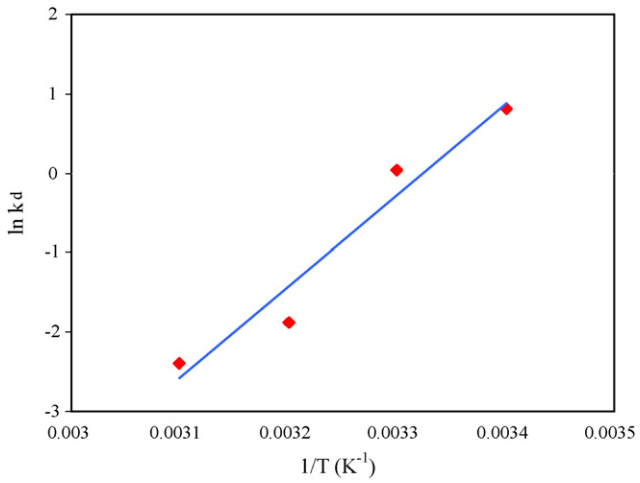

Fig. 6. Vant Hoff plot for lead biosorption. Initial conc. = 100 mg l^{-1}, 0.5 g in 100 ml, T = 20–50 °C, 200 rpm, 1 h.

3.2.4. Biosorption kinetics

In order to study the kinetics of biosorption process pseudo first order and second order kinetics models were applied. The pseudo second order model gave better correlation of data.

The equation of pseudo second order model is [18]

$$\frac{dq_t}{dt} = k(q_e - q_t)^2 \quad (5)$$

Integrating and rearranging Eq. (5) to a linear form as

$$\frac{t}{q_t} = \frac{1}{kq_e^2} + \frac{1}{q_e}t \quad (6)$$

where k is the rate constant of pseudo second order kinetics model, q_e is the equilibrium biosorption capacity and q_t is the biosorption capacity at any time t. A straight line plot of t versus t/q_t with correlation coefficient of 0.99, showed the validity of pseudo second order model. The applicability of pseudo second order kinetics model suggested that the lead biosorption to FRLs was based on chemical reaction, involving the exchange of electrons between biosorbent and metal. The reaction rate constant, k and equilibrium biosorption capacity, q_e were determined from the slope and intercept of the straight line plot and are presented in Table 2. The values of equilibrium capacity shown in Table 2, were in close agreement with those determined experimentally. A comparison of the pseudo second order model with experimental data is revealed in Fig. 3.

3.2.5. Biosorption thermodynamics

The solution temperature was varied in the range of 20–50 °C, keeping all other parameters constant. It was found that removal capacity decreased with increasing temperature from 25 to 50 °C. The maximum removal was achieved at 25 °C. The biosorption equilibrium constant, k_d can be described thermodynamically as [30,31]

$$\ln k_d = \frac{-\Delta H}{RT} + \frac{\Delta S}{R} \quad (7)$$

The Gibbs free energy change is given by the following equation:

$$\Delta G = -RT \ln k_d \quad (8)$$

where ΔH, ΔS, ΔG are the change in enthalpy, entropy, Gibbs free energy of the system, respectively. T is the absolute temperature (K), R is the gas constant (8.314 J mol^{-1} K^{-1}) and k_d is the equilibrium constant given by [31].

$$k_d = \frac{q_e}{C_e} \quad (9)$$

The values of k_d (l g^{-1}) were calculated at different temperatures, in the range of 20–50 °C. Reciprocal of temperature ($1/T$) was plotted against ln k_d and straight line was fitted to the data. The values of ΔH and ΔS were evaluated from the slope and intercept of the line in Fig. 6. The values of ΔG were calculated from Eq. (8). The values of ΔH, ΔS and ΔG are given in Table 2. The enthalpy change for lead was negative and a decrease in removal capacity was observed, with increasing temperature from 25 to 50 °C. The decrease in enthalpy was in conformity with exothermic and spontaneous nature of the biosorption process. Increase in value of ΔG with increase in temperature showed reduction in spontaneous nature of biosorption. The low value of ΔS implied that there was no remarkable change in the entropy as result of lead biosorption. The negative value of ΔS showed the decrease in randomness of system. The distribution of lead ions in solution was obviously more disordered compared to lead ions bound to the biosorbent surface and this resulted in net decrease in entropy.

3.2.6. Comparison of FRLs with other sorbents

Table 3 summaries the comparison of the maximum biosorption capacities of various sorbents including FRLs. This comparison shows that FRLs has higher biosorption capacities than oryza sativa L. husk [22], rice husk ash [32], coir [33], Aspergilus niger [34], Caulerpa lentillifera [35], papaya wood [36], olive pomace [37], jute, saw dust, groundnut shells [38] and waste tea leaves [39]. Sago waste [14] has higher biosorption capacity than FRLs. The easy availability and cost effectiveness of FRLs biomass are additional advantages, which make it better biosorbent for treatment of lead wastes.

Table 3
Comparison of maximum biosorption capacity of FRLs with other sorbents.

Biosorbent	q_{max} (mg g^{-1})	pH	Reference
Caulerpa lentillifera	29.0	5.0	[35]
Oryza sativa L. husk	8.6	5.0	[22]
Rice husk ash	12.6	5.6–5.8	[32]
Coir	18.9	5.5	[33]
Aspergilus niger	10.1	5.0	[34]
Sago waste	46.6	4.5–5.0	[14]
Papaya wood	17.4	5.0	[36]
Olive pomace	7.0	5.0	[37]
Jute	17.2	–	[38]
Sawdust	12.6	–	[38]
Groundnut shells	12.2	–	[38]
Waste tea leaves	2.1	–	[39]
FRLs	37.5	4.0	This work

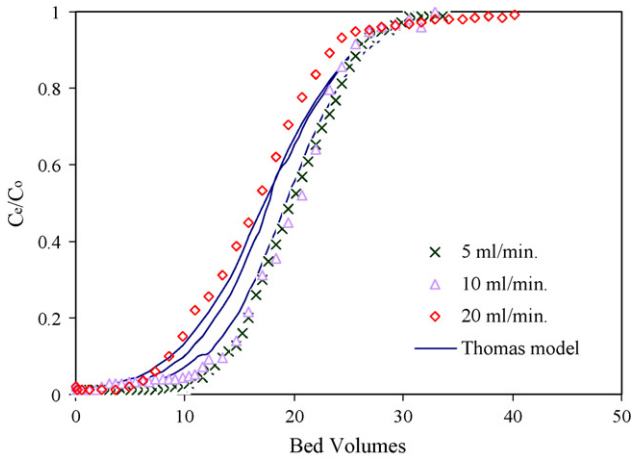

Fig. 7. Effect of flow rate on breakthrough curves. Initial conc. = 100 mg l^{-1}, 25 °C, pH 5.1, flow rate = 5–20 ml min^{-1}.

3.3. Continuous biosorption in packed column

Batch biosorption studies provide information on biosorption equilibrium and kinetics. For practical applications of biosorption process, continuous flow experiments are essential and these were conducted in fixed bed columns. This type of arrangement makes efficient utilization of the concentration gradient between the metal biosorbed and its portion remaining in the solution. The overall performance of the column is judged by its service time which is defined as the time, until the biosorbed metal breaks through the column bed and is detected in the column effluent. At that time column is considered to be saturated and must be regenerated. The column performance was studied by varying the flow rate, bed height and solution pH.

3.3.1. Effect of flow rate

Flow rate is an important characteristic in evaluating the performance of biosorption, for continuous treatment of wastewater on industrial scale. The effect of flow rate on lead biosorption was studied by varying the flow rate from 5 to 20 ml min^{-1}, while the bed height and initial metal concentration were held constant at 50 cm and 100 mg l^{-1}, respectively. The experimental breakthrough curves are shown in Fig. 7. The column performed well at the lowest flow rate. An earlier breakthrough and exhaustion times were achieved, when the flow rate was increased from 5 to 20 ml min^{-1}. The column breakthrough time was reduced from 39 to 6 h, with the increase in flow rate from 5 to 20 ml min^{-1}. This behavior was due to the decrease in the residence time, which restricted the contact of metal solution to the biosorbent. At higher flow rates the metals ions did not have enough time to diffuse into the pores of the biosorbent and they leave the column before equilibrium occurred. Due to this reason column exhaustion time was reduced. This resulted in low metal uptake and least percentage removal at higher flow rates. As the flow rate increases, metal concentration in the effluent increased rapidly resulting in sharper breakthrough curves. At lower flow rates the residence time of the metal solution in the column was increased and metal ions have more time to diffuse into the pores of biosorbent through intra-particle diffusion.

Successful design of a column biosorption process required prediction of the concentration time profile. Various mathematical models have been used to describe the fixed bed biosorption. Among these, the Thomas model is simple and widely used by several investigators [35,40]. The Thomas model, assumes the Langmuir kinetics of sorption desorption, with no axial dispersion. It is derived with the assumption that the rate driving force in sorption obeys second order reversible reaction kinetics. The Thomas model also assumes a constant separation factor but it is applicable to either favorable or unfavorable isotherms [41].

The Thomas model has the following form:

$$\frac{C_e}{C_o} = \frac{1}{1 + \exp((k_{th}/Q)(q_o M - C_o V_{eff}))} \quad (10)$$

Eq. (10) can be expressed in linear form as

$$\ln\left[\frac{C_o}{C_e} - 1\right] = \frac{k_{th} q_o M}{Q} - k_{th} C_o t \quad (11)$$

$$V_{eff} = Q t \quad (12)$$

where V_{eff} is the volume of effluent (l), k_{th} is the Thomas model constant (l mg^{-1} h^{-1}), q_o is the biosorption capacity (mg g^{-1}), Q is the volumetric flow rate through column (l h^{-1}), M is the mass of biosorbent in the column (g), C_o is the initial metal concentration (mg g^{-1}) and C_e is the effluent metal concentration (mg g^{-1}) at any time, t (h). The Thomas model constants k_{th} and q_o were determined from plot of $\ln[C_o/C_e - 1]$ versus t, at a given flow rate. The Thomas model gave a good fit of the experimental data, at all the flow rates examined, with high correlation coefficients of greater than 0.94. The comparison between experimental and the Thomas model predicted breakthrough curves is shown in Fig. 7. There was a negligible difference between the experimental and model predicted breakthrough curves at 20 ml min^{-1} but at lower flow rates a little deviation of the Thomas model from experimental data was observed. This deviation may be due to the dominance of intra-particle diffusion mechanism at lower flow rates. The values of the Thomas model parameters are presented in Table 2. These values showed that bed capacity q_o decreased with increasing flow rate, while the Thomas model constant k_{th} increased with increasing flow rate from 5 to 20 ml min^{-1}.

3.3.2. Effect of bed height

The uptake of metals in fixed bed column is dependent on the quantity of biosorbent in the column. The experiments were performed, at three different bed heights of 30, 40 and 50 cm, achieved by packing 70.7, 94.5 and 118.2 g immobilized FRLs in the column, respectively. The flow rate and initial metal concentration were kept constant at 10 ml min^{-1} and 100 mg l^{-1}, respectively. As depicted by Fig. 8 the breakthrough time varied with bed height. Steeper breakthrough curves were achieved with decrease in bed depth. The breakthrough time decreased from 18 to 6.5 h, with decreasing bed depth from 50 to 30 cm, as binding sites were restricted at low bed depths. More over at low bed depths, the axial dispersion

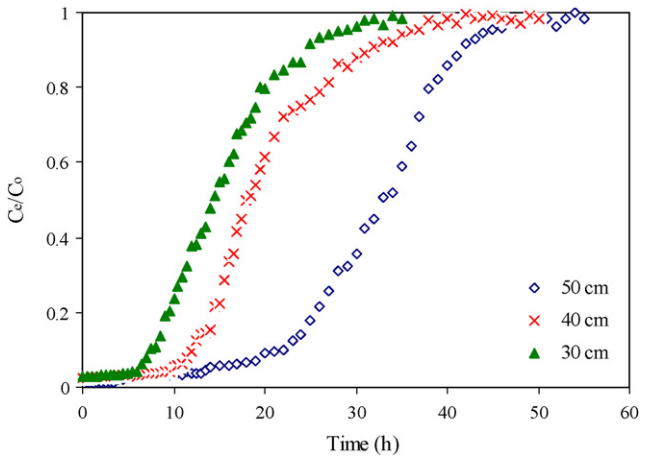

Fig. 8. Effect of bed depth on breakthrough curves. Flow rate = 10 ml min^{-1}, 25 °C, pH 5.1, initial conc. = 100 mg l^{-1}.

phenomenon predominate in mass transfer and reduce the diffusion of metal ions. The metal ions do not have enough time to diffuse into the whole of the biosorbent mass, due to which reduction in breakthrough time occurred. With the increase in bed depth, the residence time of solution in the column was increased, allowing the metal ions to diffuse deeper inside the biosorbent. The volume of metal solution treated also increased with increasing bed depth.

The BDST is a simple model for predicting the relationship between bed depth and service time in terms of process concentrations and biosorption parameters. The model is based on physically measuring the capacity of the bed at different breakthrough values. It ignores the intra-particle mass transfer resistance and external film resistance such that the sorbate is sorbed onto the biosorbent surface directly [42]. It states that the bed height, Z and service time, t of a column bears a linear relationship. The rate of sorption is controlled by the surface reaction between sorbate and unused capacity of the biosorbent.

The equation of the BDST model can be expressed in linear form as

$$t = \frac{N_o Z}{C_o v} - \frac{1}{C_o k_a} \ln\left[\frac{C_o}{C_e} - 1\right] \quad (13)$$

where N_o is the biosorption capacity of bed (mg l^{-1}), v is the linear flow velocity of metal solution through the bed (ml cm^{-2} h^{-1}) and k_a is the rate constant (l mg^{-1} h^{-1}), which characterizes the rate of solute transfer from the fluid phase to the solid phase [40]. The column service time was selected as the time when the effluent metal concentration reached 5 mg l^{-1}. The plot of service time versus bed depth, at flow rate of 10 ml min^{-1} (Fig. 9) was linear. The correlation coefficient of 0.98 indicated the validity of the BDST model for the present system. The value of N_o and k_a were evaluated from the slope and intercept of the BDST plot, assuming that initial metal concentration, C_o and linear velocity, v remained constant during the column operation. The values of BDST model parameters are presented in Table 2. The value of k_a is useful to describe the capacity of biosorption column. If k_a is large, even a short bed will avoid breakthrough, but as k_a decreases a longer bed is required [40]. The BDST model parameters are used to scale up the biosorption process for other flow rates without further experimental run.

3.3.3. Effect of pH

The most important parameter, influencing the biosorption capacity is the solution pH. The inlet pH of the metal solution is related to the biosorption mechanism onto the biosorbent surface and reflects the nature of the physico-chemical interaction of the species in the solution and on effective sites of biosorbent. The biosorption process was studied by varying the solution pH from 2 to 5. The breakthrough curves are shown in Fig. 10. The break through curves became steeper with the decrease in pH from 4 to 2 and with increase in pH from 4 to 5. The decrease in breakthrough and exhaustion time was observed with decrease in pH from 4 to 2. The pH dependence of metal biosorption can largely be related to the type and ionic state of the functional groups present in the biosorbent. As can be seen from the FTIR spectra of biomass (Fig. 1), the most of the functional groups present in FRLs biomass are acidic. These groups are positively charged at lower pH and restrict the sorption of positive cations like lead(II) due to electrostatic repulsion. As pH is increased these become negatively charged and attract lead(II) cations. When pH was further increased above 5 the sorption was reduced due to formation of lead hydroxide.

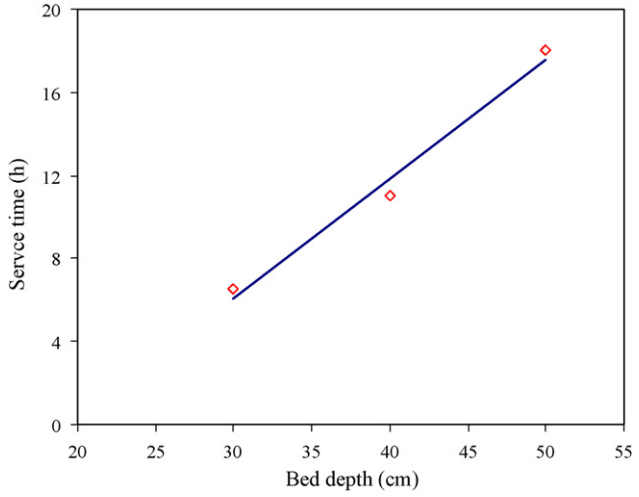

Fig. 9. BDST plot for lead biosorption.

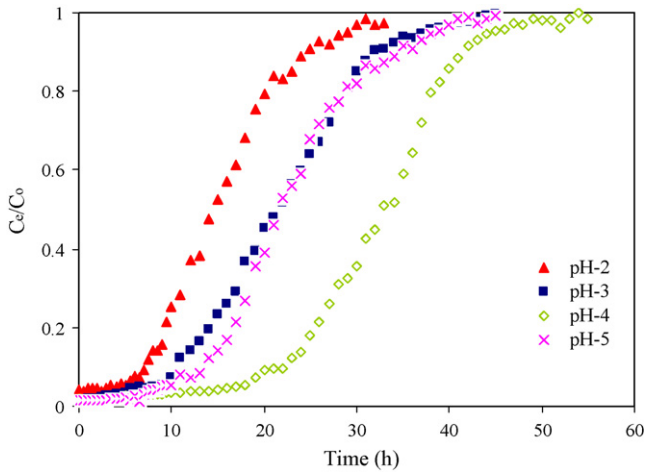

Fig. 10. Effect of pH on breakthrough curves. Flow rate = 10 ml min^{-1}, 26.3 °C, bed height = 50 cm, initial conc. = 100 mg l^{-1}.

3.3.4. Release of light metals

As a result of lead biosorption, the release of light metals like Ca, Mg, Na and K was observed in the column effluents. The elemental analysis of FRLs indicated the presence of these light metals in the biomass structure. These metals were release in exchange with the lead binding to the biomass. The release was in the following

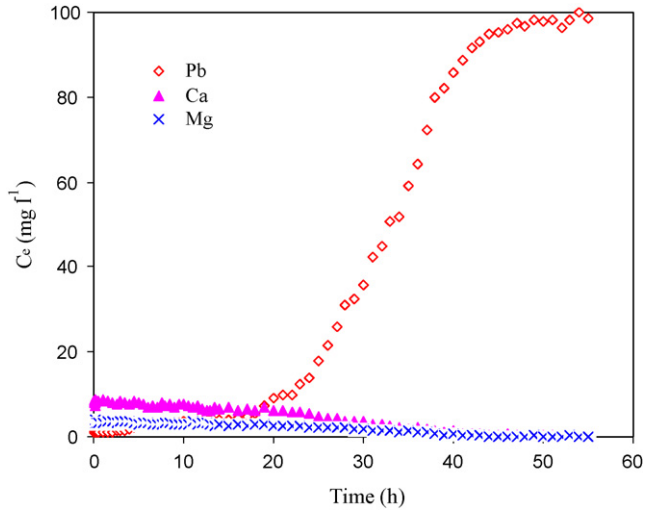

Fig. 11. Release of calcium and magnesium ions as result of lead biosorption. Flow rate = 10 ml min^{-1}, 25.4 °C, bed height = 50 cm, initial conc. of lead = 100 mg l^{-1}.

order: Ca > Mg > K > Na. The release of Ca and Mg ions as result of lead uptake is illustrated in Fig. 11.

3.3.5. Regeneration of biomass

The regeneration of biosorbent is vital, if the biosorption is to be employed for treatment of industrial wastewater. The biosorbed lead metal was recovered, from FRLs biomass by treating it with 0.05 M HNO_3 solution. About 88% of metal was recovered. The regenerated biomass was reused for further cycles of biosorption in batch mode. After five cycles of sorption–desorption, 45% loss in efficiency of FRLs biomass was observed.

The column regeneration studies were carried out for five sorption–desorption cycles. The desorption of lead was achieved by passing 0.05 M HNO_3 solution at flow rate of 10 ml min^{-1}. A negligible loss in bed height and mass of biomass beads was observed after five cycles. The elution efficiencies were greater than 96% and biosorption capacity remained almost constant irrespective of the number of cycles.

4. Conclusions

This study identified that FRLs in free and immobilized form could be used as potential sorbent, for the removal of lead from wastewater. The biosorption has been found to be spontaneous and relatively fast. The maximum biosorption capacity of lead was 37.45 mg g^{-1} at pH of 4. The temperature has strong influence on biosorption and the maximum removal was observed at 25 °C. The pseudo second order and the Langmuir isotherm models were found, the most appropriate to describe the kinetics and equilibrium of the biosorption process, respectively. The column breakthrough curves were analyzed at different flow rates, pH and bed depth. The Thomas model was reasonably accurate in predicting experimental column results for this work. The ion exchange was the principal removal mechanism, whereby metals originally attached onto the biomass structure were replaced by lead cations. The biomass was easily regenerated by passing 0.05 M HNO_3 solution through column and was reused for five sorption–desorption cycles without any considerable loss in biosorption capacity.

Acknowledgement

Authors are grateful to Higher Education Commission of Pakistan for funding this research.

References

[1] B. Volesky, Z. Holan, Biosorption of heavy metals, Biotechnol. Prog. 11 (1995) 235–250.
[2] M. Nadeem, A. Mahmood, S.A. Shahid, S.S. Shah, A.M. Khalid, G. Mckay, Sorption of lead from aqueous solution by chemically modified carbon adsorbents, J. Hazard. Mater. B138 (2006) 604–613.
[3] C. Raji, T.S. Anirudhan, Chromium(VI) adsorption by sawdust carbon: kinetics and equilibrium, Indian J. Chem. Technol. 4 (1997) 228–236.
[4] A. Ornek, M. Ozacar, I.A. Sengil, Adsorption of lead onto formaldehyde or sulphuric acid treated acorn waste: equilibrium and kinetic studies, Biochem. Eng. J. 37 (2007) 192–200.
[5] V.K. Gupta, A. Rastogi, Biosorption of lead from aqueous solutions by green algae Spirogyra species: kinetics and equilibrium studies, J. Hazard. Mater. 152 (2008) 407–414.
[6] Y.H. Wang, S.H. Lin, R.S. Juang, Removal of heavy metal ions from aqueous solutions using various low-cost adsorbents, J. Hazard. Mater. B102 (2003) 291–302.
[7] Y.C. Sharma, Cr(VI) removal from industrial effluents by adsorption on an indigenous low cost material, Colloids Surf. A: Physicochem. Eng. Aspects 215 (2003) 155–162.
[8] D. Kratochvil, B. Volesky, Advances in the biosorption of heavy metals, Trends Biotechnol. 16 (1998) 291–300.
[9] D.P. Mungasavalli, T. Viraraghavan, Y.C. Jin, Biosorption of chromium from aqueous solutions by pretreated *Aspergillus niger*: batch and column studies, Colloids Surf. A: Physicochem. Eng. Aspects 301 (2007) 214–223.
[10] W.T. Tan, S.T. Ool, C.K. Lee, Removal of Cr(VI) from solution by coconut husk and palm pressed fibres, Environ. Technol. 14 (1993) 277–282.
[11] O.S. Amuda, A.A. Giwa, I.A. Bello, Removal of heavy metal from industrial wastewater using modified activated coconut shell carbon, Biochem. Eng. J. 36 (2007) 174–181.
[12] D. Kratochvil, P. Pimentel, B. Volesky, Removal of trivalent and hexavalent chromium by seaweed biosorbent, Environ. Sci. Technol. 32 (1998) 2693–2698.
[13] R. Senthilkumar, K. Vijayaraghavan, M. Thilakavathi, P.V.R. Iyer, M. Velan, Application of seaweeds for the removal of lead from aqueous solution, Biochem. Eng. J. 33 (2007) 211–216.
[14] S.Y. Quek, D.A. Wase, C.F. Forster, The use of sago waste for the sorption of lead and copper, Water SA 24 (1998) 251–256.
[15] G. Cimino, A. Passerini, G. Toscano, Removal of toxic cations and Cr(VI) from aqueous solution by hazelnut shell, Water Res. 34 (2000) 2955–2962.
[16] Y. Bulut, Z. Tez, Adsorption studies on ground shells of hazelnut and almond, J. Hazard. Mater. 149 (2007) 35–41.
[17] P. Brown, A. Jefcoat, D. Parrish, S. Gill, E. Graham, Evaluation of the adsorptive capacity of peanut hull pellets for heavy metals in solution, Adv. Environ. Res. 4 (2000) 19–29.
[18] Y.S. Ho, Effect of pH on lead removal from water using tree fern as the sorbent, Bioresour. Technol. 96 (2005) 1292–1296.
[19] A. Saeed, M. Iqbal, M.W. Akhtar, Removal and recovery of lead(II) from single and multi metal (Cd, Cu, Ni, Zn) solutions by crop milling waste (black gram husk), J. Hazard. Mater. 117 (2005) 65–73.
[20] N.A.A. Babarinde, J.O. Babalola, R.A. Sanni, Biosorption of lead ions from aqueous solution by maize leaf, Int. J. Phys. Sci. 1 (2006) 23–26.
[21] Y. Zhang, C. Banks, A comparison of the properties of polyurethane immobilized Sphagnum moss, seaweed, sunflower waste and maize for the biosorption of Cu, Pb, Zn and Ni in continuous flow packed columns, Water Res. 40 (2006) 788–798.
[22] M.M.D. Zulkali, A.L. Ahmad, N.H. Norulakmal, Oryza sativa L. husk as heavy metal adsorbent: optimization with lead as model solution, Bioresour. Technol. 97 (2006) 21–25.
[23] K. Kaikake, K. Hoaki, H. Sunada, R.P. Dhakal, Y. Baba, Removal characteristics of metal ions using degreased coffee beans: adsorption equilibrium of cadmium(II), Bioresour. Technol. 98 (2007) 2787–2791.
[24] S. Qaiser, A.R. Saleemi, M.M. Ahmad, Heavy metal uptake by agro based waste materials, Electronic J. Biotechnol. 10 (2007) 409–416.
[25] A. Ozer, Removal of Pb(II) ions from aqueous solutions by sulphuric acid-treated wheat bran, J. Hazard. Mater. 141 (2007) 753–761.
[26] B.M.W.P.K. Amarasinghe, R.A. Williams, Tea waste as a low cost adsorbent for the removal of Cu and Pb from wastewater, Chem. Eng. J. 132 (2007) 299–309.
[27] E.M. Trujillo, T.H. Jaffers, C. Ferguson, H.Q. Stevenson, Mathematically modeling the removal of heavy metals from a wastewater using immobilized biomass, Environ. Sci. Technol. 25 (1991) 1559–1565.
[28] M.R. Sangi, A. Shahmoradi, J. Zolgharnein, G.H. Azimi, M. Ghorbandoost, Removal and recovery of heavy metals from aqueous solution using *Ulmus carpinifolia* and *Fraxinus excelsior* tree leaves, J. Hazard. Mater. 155 (2008) 513–522.
[29] B. Volesky, Sorption and Biosorption, BV Sorbex Inc., Montreal-St. Lambert, Quebec, Canada, 2003, ISBN 0-9732983-0-8.
[30] S.Q. Memon, N. Memon, S.W. Shah, M.Y. Khuhawar, M.I. Bhanger, Sawdust-A green and economical sorbent for the removal of cadmium(II) ions, J. Hazard. Mater. B139 (2007) 116–121.
[31] N. Bektas, B.A. Agim, S. Kara, Kinetic and equilibrium studies in removing lead ions from aqueous solution by natural sepiolite, J. Hazard. Mater. B112 (2004) 115–122.
[32] Q. Feng, Q. Lin, F. Gong, S. Sugita, M. Shoya, Adsorption of lead and mercury by rice husk ash, J. Colloid Interface Sci. 278 (2004) 1–8.
[33] K. Conrad, H.C.B. Hansen, Sorption of zinc and lead on coir, Bioresour. Technol. 98 (2007) 89–97.
[34] A. Kapoor, T. Viraragharan, R.D. Cullimore, Removal of heavy metals using the fungus *Aspergillus niger*, Bioresour. Technol. 70 (1999) 95–104.
[35] R. Apiratikul, P. Pavasant, Batch and column studies of biosorption of heavy metals by *Caulerpa lentillifera*, Bioresour. Technol. 99 (2008) 2766–2777.
[36] A. Saeed, M.W. Akhtar, M. Iqbal, Removal and recovery of heavy metals from aqueous solution using papaya wood as a new biosorbent, Sep. Purif. Technol. 45 (2005) 25–31.
[37] F. Pagnanelli, S. Mainelli, F. Veglio, L. Toro, Heavy metal removal by olive pomace: biosorbent characterization and equilibrium modelling, Chem. Eng. Sci. 58 (2003) 4709–4717.
[38] S.R. Shukla, R.S. Pai, Removal of Pb(II) from solution using cellulose containing materials, J. Chem. Technol. Biotechnol. 80 (2005) 176–183.
[39] S.S. Ahluwalia, D. Goyal, Removal of heavy metals by waste tea leaves from aqueous solution, Eng. Life Sci. 5 (2005) 158–162.
[40] K. Vijayaraghavana, J. Jeganb, K. Palaniveluc, M. Velana, Batch and column removal of copper from aqueous solution using a brown marine alga *Turbinaria ornate*, Chem. Eng. J. 106 (2005) 177–184.
[41] E. Malkoc, Y. Nuhoglu, Fixed bed studies for the sorption of chromium(VI) onto tea factory waste, Chem. Eng. Sci. 61 (2006) 4363–4372.
[42] D.C.K. Ko, J.F. Porter, G. McKay, Optimized correlations for the fixed-bed adsorption of metal ions on bone char, Chem. Eng. Sci. 55 (2000) 5819–5829.